Simultaneous Measurement of the Ratio $R = \mathcal{B}(t \to Wb)/\mathcal{B}(t \to Wq)$ and the Top-Quark Pair Production Cross Section with the D0 Detector at $\sqrt{s} = 1.96$ TeV

V. M. Abazov,[36] B. Abbott,[76] M. Abolins,[66] B. S. Acharya,[29] M. Adams,[52] T. Adams,[50] E. Aguilo,[6] S. H. Ahn,[31] M. Ahsan,[60] G. D. Alexeev,[36] G. Alkhazov,[40] A. Alton,[65,*] G. Alverson,[64] G. A. Alves,[2] M. Anastasoaie,[35] L. S. Ancu,[35] T. Andeen,[54] S. Anderson,[46] B. Andrieu,[17] M. S. Anzelc,[54] Y. Arnoud,[14] M. Arov,[61] M. Arthaud,[18] A. Askew,[50] B. Åsman,[41] A. C. S. Assis Jesus,[3] O. Atramentov,[50] C. Autermann,[21] C. Avila,[8] C. Ay,[24] F. Badaud,[13] A. Baden,[62] L. Bagby,[53] B. Baldin,[51] D. V. Bandurin,[60] S. Banerjee,[29] P. Banerjee,[29] E. Barberis,[64] A.-F. Barfuss,[15] P. Bargassa,[81] P. Baringer,[59] J. Barreto,[2] J. F. Bartlett,[51] U. Bassler,[18] D. Bauer,[44] S. Beale,[6] A. Bean,[59] M. Begalli,[3] M. Begel,[72] C. Belanger-Champagne,[41] L. Bellantoni,[51] A. Bellavance,[51] J. A. Benitez,[66] S. B. Beri,[27] G. Bernardi,[17] R. Bernhard,[23] I. Bertram,[43] M. Besançon,[18] R. Beuselinck,[44] V. A. Bezzubov,[39] P. C. Bhat,[51] V. Bhatnagar,[27] C. Biscarat,[20] G. Blazey,[53] F. Blekman,[44] S. Blessing,[50] D. Bloch,[19] K. Bloom,[68] A. Boehnlein,[51] D. Boline,[63] T. A. Bolton,[60] G. Borissov,[43] T. Bose,[78] A. Brandt,[79] R. Brock,[66] G. Brooijmans,[71] A. Bross,[51] D. Brown,[82] N. J. Buchanan,[50] D. Buchholz,[54] M. Buehler,[82] V. Buescher,[22] V. Bunichev,[38] S. Burdin,[43,†] S. Burke,[46] T. H. Burnett,[83] C. P. Buszello,[44] J. M. Butler,[63] P. Calfayan,[25] S. Calvet,[16] J. Cammin,[72] W. Carvalho,[3] B. C. K. Casey,[51] N. M. Cason,[56] H. Castilla-Valdez,[33] S. Chakrabarti,[18] D. Chakraborty,[53] K. M. Chan,[56] K. Chan,[6] A. Chandra,[49] F. Charles,[19,¶] E. Cheu,[46] F. Chevallier,[14] D. K. Cho,[63] S. Choi,[32] B. Choudhary,[28] L. Christofek,[78] T. Christoudias,[44,¶] S. Cihangir,[51] D. Claes,[68] Y. Coadou,[6] M. Cooke,[81] W. E. Cooper,[51] M. Corcoran,[81] F. Couderc,[18] M.-C. Cousinou,[15] S. Crépé-Renaudin,[14] D. Cutts,[78] M. Ćwiok,[30] H. da Motta,[2] A. Das,[46] G. Davies,[44] K. De,[79] S. J. de Jong,[35] E. De La Cruz-Burelo,[65] C. De Oliveira Martins,[3] J. D. Degenhardt,[65] F. Déliot,[18] M. Demarteau,[51] R. Demina,[72] D. Denisov,[51] S. P. Denisov,[39] S. Desai,[51] H. T. Diehl,[51] M. Diesburg,[51] A. Dominguez,[68] H. Dong,[73] L. V. Dudko,[38] L. Duflot,[16] S. R. Dugad,[29] D. Duggan,[50] A. Duperrin,[15] J. Dyer,[66] A. Dyshkant,[53] M. Eads,[68] D. Edmunds,[66] J. Ellison,[49] V. D. Elvira,[51] Y. Enari,[78] S. Eno,[62] P. Ermolov,[38] H. Evans,[55] A. Evdokimov,[74] V. N. Evdokimov,[39] A. V. Ferapontov,[60] T. Ferbel,[72] F. Fiedler,[24] F. Filthaut,[35] W. Fisher,[51] H. E. Fisk,[51] M. Ford,[45] M. Fortner,[53] H. Fox,[23] S. Fu,[51] S. Fuess,[51] T. Gadfort,[71] C. F. Galea,[35] E. Gallas,[51] E. Galyaev,[56] C. Garcia,[72] A. Garcia-Bellido,[83] V. Gavrilov,[37] P. Gay,[13] W. Geist,[19] D. Gelé,[19] C. E. Gerber,[52] Y. Gershtein,[50] D. Gillberg,[6] G. Ginther,[72] N. Gollub,[41] B. Gómez,[8] A. Goussiou,[56] P. D. Grannis,[73] H. Greenlee,[51] Z. D. Greenwood,[61] E. M. Gregores,[4] G. Grenier,[20] Ph. Gris,[13] J.-F. Grivaz,[16] A. Grohsjean,[25] S. Grünendahl,[51] M. W. Grünewald,[30] J. Guo,[73] F. Guo,[73] P. Gutierrez,[76] G. Gutierrez,[51] A. Haas,[71] N. J. Hadley,[62] P. Haefner,[25] S. Hagopian,[50] J. Haley,[69] I. Hall,[66] R. E. Hall,[48] L. Han,[7] P. Hansson,[41] K. Harder,[45] A. Harel,[72] R. Harrington,[64] J. M. Hauptman,[58] R. Hauser,[66] J. Hays,[44] T. Hebbeker,[21] D. Hedin,[53] J. G. Hegeman,[34] J. M. Heinmiller,[52] A. P. Heinson,[49] U. Heintz,[63] C. Hensel,[59] K. Herner,[73] G. Hesketh,[64] M. D. Hildreth,[56] R. Hirosky,[82] J. D. Hobbs,[73] B. Hoeneisen,[12] H. Hoeth,[26] M. Hohlfeld,[22] S. J. Hong,[31] S. Hossain,[76] P. Houben,[34] Y. Hu,[73] Z. Hubacek,[10] V. Hynek,[9] I. Iashvili,[70] R. Illingworth,[51] A. S. Ito,[51] S. Jabeen,[63] M. Jaffré,[16] S. Jain,[76] K. Jakobs,[23] C. Jarvis,[62] R. Jesik,[44] K. Johns,[46] C. Johnson,[71] M. Johnson,[51] A. Jonckheere,[51] P. Jonsson,[44] A. Juste,[51] E. Kajfasz,[15] A. M. Kalinin,[36] J. R. Kalk,[66] J. M. Kalk,[61] S. Kappler,[21] D. Karmanov,[38] P. A. Kasper,[51] I. Katsanos,[71] D. Kau,[50] R. Kaur,[27] V. Kaushik,[79] R. Kehoe,[80] S. Kermiche,[15] N. Khalatyan,[51] A. Khanov,[77] A. Kharchilava,[70] Y. M. Kharzheev,[36] D. Khatidze,[71] T. J. Kim,[31] M. H. Kirby,[54] M. Kirsch,[21] B. Klima,[51] J. M. Kohli,[27] J.-P. Konrath,[23] V. M. Korablev,[39] A. V. Kozelov,[39] D. Krop,[55] T. Kuhl,[24] A. Kumar,[70] S. Kunori,[62] A. Kupco,[11] T. Kurča,[20] J. Kvita,[9] F. Lacroix,[13] D. Lam,[56] S. Lammers,[71] G. Landsberg,[78] P. Lebrun,[20] W. M. Lee,[51] A. Leflat,[38] F. Lehner,[42] J. Lellouch,[17] J. Leveque,[46] J. Li,[79] Q. Z. Li,[51] L. Li,[49] S. M. Lietti,[5] J. G. R. Lima,[53] D. Lincoln,[51] J. Linnemann,[66] V. V. Lipaev,[39] R. Lipton,[51] Y. Liu,[7,¶] Z. Liu,[6] A. Lobodenko,[40] M. Lokajicek,[11] P. Love,[43] H. J. Lubatti,[83] R. Luna,[3] A. L. Lyon,[51] A. K. A. Maciel,[2] D. Mackin,[81] R. J. Madaras,[47] P. Mättig,[26] C. Magass,[21] A. Magerkurth,[65] P. K. Mal,[56] H. B. Malbouisson,[3] S. Malik,[68] V. L. Malyshev,[36] H. S. Mao,[51] Y. Maravin,[60] B. Martin,[14] R. McCarthy,[73] A. Melnitchouk,[67] L. Mendoza,[8] P. G. Mercadante,[5] M. Merkin,[38] K. W. Merritt,[51] J. Meyer,[22,§] A. Meyer,[21] T. Millet,[20] J. Mitrevski,[71] J. Molina,[3] R. K. Mommsen,[45] N. K. Mondal,[29] R. W. Moore,[6] T. Moulik,[59] G. S. Muanza,[20] M. Mulders,[51] M. Mulhearn,[71] O. Mundal,[22] L. Mundim,[3] E. Nagy,[15] M. Naimuddin,[51] M. Narain,[78] N. A. Naumann,[35] H. A. Neal,[65] J. P. Negret,[8] P. Neustroev,[40] H. Nilsen,[23] H. Nogima,[3] S. F. Novaes,[5] T. Nunnemann,[25] V. O'Dell,[51] D. C. O'Neil,[6] G. Obrant,[40] C. Ochando,[16] D. Onoprienko,[60] N. Oshima,[51] J. Osta,[56] R. Otec,[10] G. J. Otero y Garzón,[51] M. Owen,[45] P. Padley,[81] M. Pangilinan,[78] N. Parashar,[57] S.-J. Park,[72] S. K. Park,[31] J. Parsons,[71] R. Partridge,[78] N. Parua,[55] A. Patwa,[74] G. Pawloski,[81] B. Penning,[23] M. Perfilov,[38] K. Peters,[45] Y. Peters,[26] P. Pétroff,[16] M. Petteni,[44] R. Piegaia,[1] J. Piper,[66] M.-A. Pleier,[22] P. L. M. Podesta-Lerma,[33,‡]

V. M. Podstavkov,[51] Y. Pogorelov,[56] M.-E. Pol,[2] P. Polozov,[37] B. G. Pope,[66] A. V. Popov,[39] C. Potter,[6] W. L. Prado da Silva,[3] H. B. Prosper,[50] S. Protopopescu,[74] J. Qian,[65] A. Quadt,[22,§] B. Quinn,[67] A. Rakitine,[43] M. S. Rangel,[2] K. Ranjan,[28] P. N. Ratoff,[43] P. Renkel,[80] S. Reucroft,[64] P. Rich,[45] J. Rieger,[55] M. Rijssenbeek,[73] I. Ripp-Baudot,[19] F. Rizatdinova,[77] S. Robinson,[44] R. F. Rodrigues,[3] M. Rominsky,[76] C. Royon,[18] P. Rubinov,[51] R. Ruchti,[56] G. Safronov,[37] G. Sajot,[14] A. Sánchez-Hernández,[33] M. P. Sanders,[17] A. Santoro,[3] G. Savage,[51] L. Sawyer,[61] T. Scanlon,[44] D. Schaile,[25] R. D. Schamberger,[73] Y. Scheglov,[40] H. Schellman,[54] T. Schliephake,[26] C. Schwanenberger,[45] A. Schwartzman,[69] R. Schwienhorst,[66] J. Sekaric,[50] H. Severini,[76] E. Shabalina,[52] M. Shamim,[60] V. Shary,[18] A. A. Shchukin,[39] R. K. Shivpuri,[28] V. Siccardi,[19] V. Simak,[10] V. Sirotenko,[51] P. Skubic,[76] P. Slattery,[72] D. Smirnov,[56] J. Snow,[75] G. R. Snow,[68] S. Snyder,[74] S. Söldner-Rembold,[45] L. Sonnenschein,[17] A. Sopczak,[43] M. Sosebee,[79] K. Soustruznik,[9] B. Spurlock,[79] J. Stark,[14] J. Steele,[61] V. Stolin,[37] D. A. Stoyanova,[39] J. Strandberg,[65] S. Strandberg,[41] M. A. Strang,[70] M. Strauss,[76] E. Strauss,[73] R. Ströhmer,[25] D. Strom,[54] L. Stutte,[51] S. Sumowidagdo,[50] P. Svoisky,[56] A. Sznajder,[3] M. Talby,[15] P. Tamburello,[46] A. Tanasijczuk,[1] W. Taylor,[6] J. Temple,[46] B. Tiller,[25] F. Tissandier,[13] M. Titov,[18] V. V. Tokmenin,[36] T. Toole,[62] I. Torchiani,[23] T. Trefzger,[24] D. Tsybychev,[73] B. Tuchming,[18] C. Tully,[69] P. M. Tuts,[71] R. Unalan,[66] S. Uvarov,[40] L. Uvarov,[40] S. Uzunyan,[53] B. Vachon,[6] P. J. van den Berg,[34] R. Van Kooten,[55] W. M. van Leeuwen,[34] N. Varelas,[52] E. W. Varnes,[46] I. A. Vasilyev,[39] M. Vaupel,[26] P. Verdier,[20] L. S. Vertogradov,[36] M. Verzocchi,[51] F. Villeneuve-Seguier,[44] P. Vint,[44] P. Vokac,[10] E. Von Toerne,[60] M. Voutilainen,[68,||] R. Wagner,[69] H. D. Wahl,[50] L. Wang,[62] M. H. L. S Wang,[51] J. Warchol,[56] G. Watts,[83] M. Wayne,[56] M. Weber,[51] G. Weber,[24] L. Welty-Rieger,[55] A. Wenger,[42] N. Wermes,[22] M. Wetstein,[62] A. White,[79] D. Wicke,[26] G. W. Wilson,[59] S. J. Wimpenny,[49] M. Wobisch,[61] D. R. Wood,[64] T. R. Wyatt,[45] Y. Xie,[78] S. Yacoob,[54] R. Yamada,[51] M. Yan,[62] T. Yasuda,[51] Y. A. Yatsunenko,[36] K. Yip,[74] H. D. Yoo,[78] S. W. Youn,[54] J. Yu,[79] A. Zatserklyaniy,[53] C. Zeitnitz,[26] T. Zhao,[83] B. Zhou,[65] J. Zhu,[73] M. Zielinski,[72] D. Zieminska,[55] A. Zieminski,[55,¶] L. Zivkovic,[71] V. Zutshi,[53] and E. G. Zverev[38]

(D0 Collaboration)

[1]*Universidad de Buenos Aires, Buenos Aires, Argentina*
[2]*LAFEX, Centro Brasileiro de Pesquisas Físicas, Rio de Janeiro, Brazil*
[3]*Universidade do Estado do Rio de Janeiro, Rio de Janeiro, Brazil*
[4]*Universidade Federal do ABC, Santo André, Brazil*
[5]*Instituto de Física Teórica, Universidade Estadual Paulista, São Paulo, Brazil*
[6]*University of Alberta, Edmonton, Alberta, Canada, Simon Fraser University, Burnaby, British Columbia, Canada, York University, Toronto, Ontario, Canada, and McGill University, Montreal, Quebec, Canada*
[7]*University of Science and Technology of China, Hefei, People's Republic of China*
[8]*Universidad de los Andes, Bogotá, Colombia*
[9]*Center for Particle Physics, Charles University, Prague, Czech Republic*
[10]*Czech Technical University, Prague, Czech Republic*
[11]*Center for Particle Physics, Institute of Physics, Academy of Sciences of the Czech Republic, Prague, Czech Republic*
[12]*Universidad San Francisco de Quito, Quito, Ecuador*
[13]*LPC, Univ Blaise Pascal, CNRS/IN2P3, Clermont, France*
[14]*LPSC, Université Joseph Fourier Grenoble 1, CNRS/IN2P3, Institut National Polytechnique de Grenoble, France*
[15]*CPPM, IN2P3/CNRS, Université de la Méditerranée, Marseille, France*
[16]*LAL, Univ Paris-Sud, IN2P3/CNRS, Orsay, France*
[17]*LPNHE, IN2P3/CNRS, Universités Paris VI and VII, Paris, France*
[18]*DAPNIA/Service de Physique des Particules, CEA, Saclay, France*
[19]*IPHC, Université Louis Pasteur et Université de Haute Alsace, CNRS/IN2P3, Strasbourg, France*
[20]*IPNL, Université Lyon 1, CNRS/IN2P3, Villeurbanne, France and Université de Lyon, Lyon, France*
[21]*III. Physikalisches Institut A, RWTH Aachen, Aachen, Germany*
[22]*Physikalisches Institut, Universität Bonn, Bonn, Germany*
[23]*Physikalisches Institut, Universität Freiburg, Freiburg, Germany*
[24]*Institut für Physik, Universität Mainz, Mainz, Germany*
[25]*Ludwig-Maximilians-Universität München, München, Germany*
[26]*Fachbereich Physik, University of Wuppertal, Wuppertal, Germany*
[27]*Panjab University, Chandigarh, India*
[28]*Delhi University, Delhi, India*
[29]*Tata Institute of Fundamental Research, Mumbai, India*
[30]*University College Dublin, Dublin, Ireland*

[31]Korea Detector Laboratory, Korea University, Seoul, Korea
[32]SungKyunKwan University, Suwon, Korea
[33]CINVESTAV, Mexico City, Mexico
[34]FOM-Institute NIKHEF and University of Amsterdam/NIKHEF, Amsterdam, The Netherlands
[35]Radboud University Nijmegen/NIKHEF, Nijmegen, The Netherlands
[36]Joint Institute for Nuclear Research, Dubna, Russia
[37]Institute for Theoretical and Experimental Physics, Moscow, Russia
[38]Moscow State University, Moscow, Russia
[39]Institute for High Energy Physics, Protvino, Russia
[40]Petersburg Nuclear Physics Institute, St. Petersburg, Russia
[41]Lund University, Lund, Sweden, Royal Institute of Technology and Stockholm University, Stockholm, Sweden, and Uppsala University, Uppsala, Sweden
[42]Physik Institut der Universität Zürich, Zürich, Switzerland
[43]Lancaster University, Lancaster, United Kingdom
[44]Imperial College, London, United Kingdom
[45]University of Manchester, Manchester, United Kingdom
[46]University of Arizona, Tucson, Arizona 85721, USA
[47]Lawrence Berkeley National Laboratory and University of California, Berkeley, California 94720, USA
[48]California State University, Fresno, California 93740, USA
[49]University of California, Riverside, California 92521, USA
[50]Florida State University, Tallahassee, Florida 32306, USA
[51]Fermi National Accelerator Laboratory, Batavia, Illinois 60510, USA
[52]University of Illinois at Chicago, Chicago, Illinois 60607, USA
[53]Northern Illinois University, DeKalb, Illinois 60115, USA
[54]Northwestern University, Evanston, Illinois 60208, USA
[55]Indiana University, Bloomington, Indiana 47405, USA
[56]University of Notre Dame, Notre Dame, Indiana 46556, USA
[57]Purdue University Calumet, Hammond, Indiana 46323, USA
[58]Iowa State University, Ames, Iowa 50011, USA
[59]University of Kansas, Lawrence, Kansas 66045, USA
[60]Kansas State University, Manhattan, Kansas 66506, USA
[61]Louisiana Tech University, Ruston, Louisiana 71272, USA
[62]University of Maryland, College Park, Maryland 20742, USA
[63]Boston University, Boston, Massachusetts 02215, USA
[64]Northeastern University, Boston, Massachusetts 02115, USA
[65]University of Michigan, Ann Arbor, Michigan 48109, USA
[66]Michigan State University, East Lansing, Michigan 48824, USA
[67]University of Mississippi, University, Mississippi 38677, USA
[68]University of Nebraska, Lincoln, Nebraska 68588, USA
[69]Princeton University, Princeton, New Jersey 08544, USA
[70]State University of New York, Buffalo, New York 14260, USA
[71]Columbia University, New York, New York 10027, USA
[72]University of Rochester, Rochester, New York 14627, USA
[73]State University of New York, Stony Brook, New York 11794, USA
[74]Brookhaven National Laboratory, Upton, New York 11973, USA
[75]Langston University, Langston, Oklahoma 73050, USA
[76]University of Oklahoma, Norman, Oklahoma 73019, USA
[77]Oklahoma State University, Stillwater, Oklahoma 74078, USA
[78]Brown University, Providence, Rhode Island 02912, USA
[79]University of Texas, Arlington, Texas 76019, USA
[80]Southern Methodist University, Dallas, Texas 75275, USA
[81]Rice University, Houston, Texas 77005, USA
[82]University of Virginia, Charlottesville, Virginia 22901, USA
[83]University of Washington, Seattle, Washington 98195, USA
(Received 10 January 2008; published 14 May 2008)

We present the first simultaneous measurement of the ratio of branching fractions, $R = \mathcal{B}(t \rightarrow Wb)/\mathcal{B}(t \rightarrow Wq)$, with q being a d, s, or b quark, and the top-quark pair production cross section $\sigma_{t\bar{t}}$ in the lepton plus jets channel using 0.9 fb^{-1} of $p\bar{p}$ collision data at $\sqrt{s} = 1.96$ TeV collected with the D0 detector. We extract R and $\sigma_{t\bar{t}}$ by analyzing samples of events with 0, 1, and ≥ 2 identified b jets. We measure $R = 0.97^{+0.09}_{-0.08}$(stat + syst) and $\sigma_{t\bar{t}} = 8.18^{+0.90}_{-0.84}$(stat + syst) $\pm$ 0.50(lumi) pb, in agreement with the standard model prediction.

DOI: 10.1103/PhysRevLett.100.192003 PACS numbers: 13.85.Lg, 12.15.Hh, 13.85.Qk, 14.65.Ha

Within the standard model (SM) the top quark decays to a W boson and a down-type quark q ($q = d$, s, b) with a rate proportional to the squared Cabibbo-Kobayashi-Maskawa (CKM) matrix element, $|V_{tq}|^2$ [1]. Under the assumption of three fermion families and a unitary 3×3 CKM matrix, the $|V_{tq}|$ elements are severely constrained, with $|V_{tb}| = 0.999100^{+0.000034}_{-0.000004}$ [2]. However, in several extensions of the SM the 3×3 CKM submatrix would not appear unitary and $|V_{tq}|$ elements can significantly deviate from their SM values. This would affect the rate for single top-quark production via the electroweak interaction [3] and the ratio R of the top-quark branching fractions, which can be expressed in terms of the CKM matrix elements as

$$R = \frac{\mathcal{B}(t \to Wb)}{\mathcal{B}(t \to Wq)} = \frac{|V_{tb}|^2}{|V_{tb}|^2 + |V_{ts}|^2 + |V_{td}|^2}.$$

A precise measurement of R is therefore a necessary ingredient for performing direct measurements of the $|V_{tq}|$ elements via the combination with future measurements of the single top-quark production in s and t channels [4], free of assumptions about the number of quark families or the unitarity of the CKM matrix.

We report the first simultaneous measurement of R and the top-quark pair ($t\bar{t}$) production cross section $\sigma_{t\bar{t}}$. R was measured by the CDF and D0 collaborations [5,6]. The simultaneous measurement of R and $\sigma_{t\bar{t}}$, in contrast to previous measurements [7,8], allows one to extract $\sigma_{t\bar{t}}$ without assuming $\mathcal{B}(t \to Wb) = 1$, and to achieve a higher precision on both quantities by exploiting their different sensitivity to systematic uncertainties.

The current measurement is based on data collected with the D0 detector [9] between August 2002 and December 2005 at the Fermilab Tevatron $p\bar{p}$ collider at $\sqrt{s} = 1.96$ TeV, corresponding to an integrated luminosity of about 0.9 fb^{-1}. We use the top-quark pair decay channel $t\bar{t} \to W^+ q W^- \bar{q}$, with the subsequent decay of one W boson into two quarks, and the other one into an electron or muon and a neutrino, referred to as the lepton plus jets (ℓ + jets) channel. We select a data sample enriched in $t\bar{t}$ events by requiring ≥ 3 jets with transverse momentum $p_T > 20$ GeV and pseudorapidity $|\eta| < 2.5$ [10], one isolated electron (muon) with $p_T > 20$ GeV and $|\eta| < 1.1$ ($|\eta| < 2.0$), and missing transverse energy $\not{E}_T > 20$ GeV (e + jets) or $\not{E}_T > 25$ GeV (μ + jets). The leading jet p_T is required to exceed 40 GeV. Events containing a second isolated lepton with $p_T > 15$ GeV are rejected. The lepton isolation criteria are based on calorimeter and tracking information. Details of lepton, jets, and $\not{E}_T$ identification are described elsewhere [10].

We identify b jets using a neural-network tagging algorithm [11]. It combines variables that characterize the presence and properties of secondary vertices and tracks with high impact parameter inside the jet. In the simulation, we assign a probability for each jet to be b tagged based on its flavor, p_T, and η. These probabilities are determined from data control samples, and can be combined to yield a probability for each $t\bar{t}$ event to have 0, 1, or ≥ 2 b-tagged jets [7].

We split the ℓ + jets sample into subsamples according to lepton flavor (e or μ), jet multiplicity (3 or ≥ 4 jets) and number of identified b jets (0, 1 or ≥ 2), thus obtaining 12 disjoint data sets. We simultaneously fit R and $\sigma_{t\bar{t}}$ to the observed number of 1 b tag and ≥ 2 b tag events, and, in 0 b tag events with ≥ 4 jets, to the shape of a discriminant $\mathcal{D}$ that exploits kinematic differences between $t\bar{t}$ signal and background. We do not use a discriminant in events with 3 jets and 0 b tags, since the signal-to-background ratio is about 5 times smaller.

The dominant background is the production of W bosons in association with heavy and light flavor jets (W + jets). Smaller contributions arise from Z + jets, diboson, and single top-quark production. Multijet events enter the selected sample if a jet is misidentified as an electron, or a muon in a jet from a heavy quark or an in-flight pion or kaon decay appears isolated.

We model W + jets and Z + jets processes with the ALPGEN [12] leading-order generator for the matrix element calculation and PYTHIA [13] for parton showering and hadronization. Diboson samples are generated with PYTHIA. Single top-quark production is modeled with the SINGLETOP [14] event generator. The $t\bar{t}$ signal is simulated with PYTHIA for a top-quark mass of $m_{\rm top} = 175$ GeV and includes three decay modes $t\bar{t} \to W^+ b W^- \bar{b}$, $t\bar{t} \to W^+ b W^- \bar{q}_l$ (or $t\bar{t} \to W^+ q_l W^- \bar{b}$) and $t\bar{t} \to W^+ q_l W^- \bar{q}_l$, where q_l denotes a light down-type (d or s) quark. These three decay modes are referred to as bb, bq_l and $q_l q_l$. We pass the generated events through a GEANT-based [15] simulation of the D0 detector. Additional corrections [10] are applied to the reconstructed objects to improve the agreement between data and simulation.

The determination of the background composition starts with the evaluation of the multijet background for each jet multiplicity and lepton flavor before b-jet tagging by counting events in the corresponding control data samples and applying the matrix method [7]. We estimate the number of events with a lepton originating from a W or Z boson decay by subtracting the multijet background from the observed event yield before b tagging. We further subtract diboson, single top quark and Z + jets contribu-

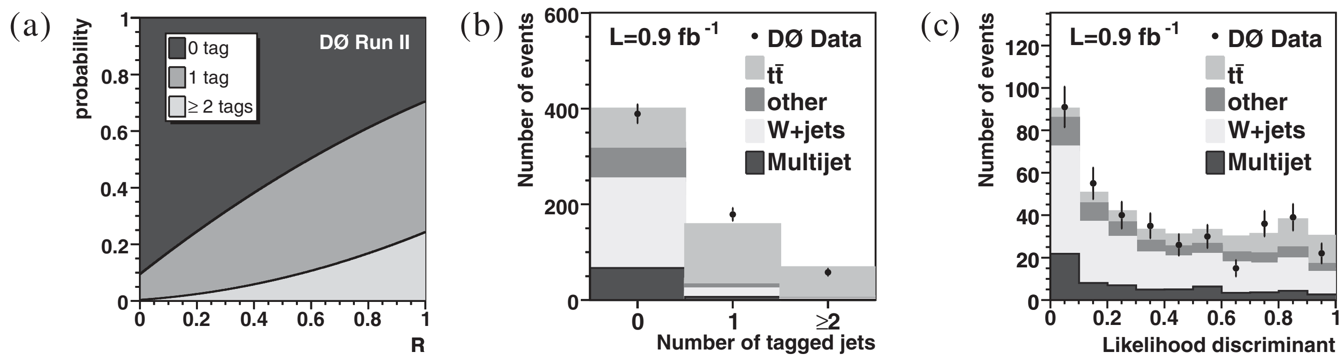

FIG. 1. (a) Probability of $t\bar{t}$ events to have 0, 1, and ≥ 2 b tags as a function of R for events with ≥ 4 jets; (b) predicted and observed number of events in the 0, 1 and ≥ 2 b tag samples for the measured R and $\sigma_{t\bar{t}}$ for events with ≥ 4 jets and (c) predicted and observed discriminant distribution in the 0 b tag sample with ≥ 4 jets.

tions, normalized to the next-to-leading-order cross sections [16]. The remaining data events are assumed to come from $t\bar{t}$ and $W +$ jets. In every step of the fitting procedure used to extract $\sigma_{t\bar{t}}$ and R, we iteratively redetermine the expected number of $t\bar{t}$ events and reevaluate the $W +$ jets background.

Since the probability to tag a $t\bar{t}$ event depends on the jet flavor, it depends on R. Assuming three $t\bar{t}$ decay modes bb, bq_l and q_lq_l, the probability for a $t\bar{t}$ event to pass our selection criteria and to have n b-tagged jets is:

$$P^n_{\text{total}}(t\bar{t}) = R^2 A(bb) P^n_t(bb) + 2R(1-R)A(bq_l)P^n_t(bq_l) + (1-R)^2 A(q_lq_l)P^n_t(q_lq_l), \tag{1}$$

where A (P^n_t) describes the acceptance (tagging probability) for each mode. Figure 1(a) shows P^n_t as a function of R for $t\bar{t}$ events with ≥ 4 jets. Table I presents the sample composition for the measured $\sigma_{t\bar{t}}$ and $R = 1$.

The topological discriminant $\mathcal{D}$ [10] exploits the kinematic differences between $t\bar{t}$ and $W +$ jets events to achieve a better constraint on the number of $t\bar{t}$ events in the subsample with ≥ 4 jets and 0 b tags. We select

TABLE I. Sample composition for the measured $\sigma_{t\bar{t}}$ and $R = 1$. Total uncertainties are given.

N_{jets}	Sample	0 b tags	1 b tag	≥ 2 b tags
3	$W +$ jets	1394.4 ± 65.1	102.5 ± 9.4	8.3 ± 1.2
	Multijet	287.4 ± 35.9	28.1 ± 3.5	3.3 ± 0.4
	Other	254.0 ± 35.2	29.4 ± 3.5	5.2 ± 0.7
	$t\bar{t}$	109.7 ± 6.6	143.3 ± 5.1	54.3 ± 4.3
	Total	2045.5 ± 82.5	303.3 ± 11.8	71.2 ± 4.5
	Observed	2050	294	76
4	$W +$ jets	188.2 ± 38.0	17.3 ± 3.8	1.8 ± 0.4
	Multijet	66.9 ± 9.9	6.6 ± 1.0	0.8 ± 0.1
	Other	62.2 ± 11.8	8.0 ± 1.4	1.7 ± 0.3
	$t\bar{t}$	83.8 ± 9.4	126.4 ± 11.4	64.2 ± 4.5
	Total	401.1 ± 42.1	158.3 ± 12.1	69.5 ± 4.5
	Observed	389	179	58

variables well described by the background model that provide a good separation between $t\bar{t}$ and $W +$ jets background. Only the four highest-p_T jets are considered for these variables to reduce the sensitivity to soft radiation. The optimal set of variables is chosen to minimize the expected statistical uncertainty on the fitted fraction of $t\bar{t}$ events. Because of differences in acceptance and sample composition, the discriminants are constructed from different sets of variables in the $e +$ jets and $\mu +$ jets channels. In the $e +$ jets channel we use five variables: the leading jet p_T, the maximum $\Delta\mathcal{R}$ [10] between two jets, $\mathcal{A}$, $\mathcal{C}_M$, and $\mathcal{D}_M$ [17]. In the $\mu +$ jets channel we use six variables: $\mathcal{A}$, $\mathcal{D}_M$, the scalar sum of the p_T of jets and the muon, the scalar sum of the p_T of the third and fourth jet, the transverse mass of all jets, and the ratio of the mass of the three leading jets to the mass of the event, defined as the invariant mass of all jets, the lepton and $\not{E}_T$.

The discriminant function is built using simulated $W +$ jets and $t\bar{t}$ events. We evaluate it for each physics process considered and build corresponding template distributions consisting of ten bins. For $t\bar{t}$ we obtain a distribution for each of the three decay modes. The shapes of the discriminant distributions for $Z +$ jets, diboson and single top backgrounds are found to be similar to that of the $W +$ jets events and we use the latter to model them. The discriminant shape for the multijet background is obtained from a sample of data events where the lepton fails the isolation criteria.

We define a likelihood function as the product of Poisson probabilities over all 30 subsamples and bins of the discriminant. In each subsample the expected number of events is estimated as a function of R and $\sigma_{t\bar{t}}$. We include 12 additional Poisson terms to constrain the multijet background in each subsample. The systematic uncertainties are incorporated in the fit using nuisance parameters [7], each represented by a Gaussian term in the likelihood. In this approach, each source of systematic uncertainty is allowed to affect the central value of R and $\sigma_{t\bar{t}}$ during the fit, yielding a combined statistical and

TABLE II. Summary of uncertainties on $\sigma_{t\bar{t}}$ and R.

Source	$\Delta\sigma_{t\bar{t}}$ (pb)	ΔR
Statistical	$+0.67 - 0.64$	$+0.067 - 0.065$
Lepton identification	$+0.32 - 0.27$	n/a
Jet energy scale	$+0.32 - 0.23$	n/a
W + jets background	$+0.21 - 0.23$	n/a
Multijet background	$+0.17 - 0.17$	$+0.016 - 0.016$
Signal modeling	$+0.12 - 0.25$	n/a
b-tagging efficiency	$+0.10 - 0.09$	$+0.059 - 0.047$
Other	$+0.24 - 0.13$	$+0.015 - 0.014$
Total uncertainty	$+0.90 - 0.84$	$+0.092 - 0.083$

systematic uncertainty. The result of the fit is

$$R = 0.97^{+0.09}_{-0.08}(\text{stat} + \text{syst}) \quad \text{and}$$
$$\sigma_{t\bar{t}} = 8.18^{+0.90}_{-0.84}(\text{stat} + \text{syst}) \pm 0.50(\text{lumi}) \text{ pb}, \tag{2}$$

for a top-quark mass of 175 GeV. Figures 1(b) and 1(c) compare the distribution of the data to the sum of predicted background and measured signal. We observe no significant dependence of R on m_{top} within ± 10 GeV around the assumed value while $\sigma_{t\bar{t}}$ changes by ∓ 0.09 pb per 1 GeV within the same range. We find a correlation between R and $\sigma_{t\bar{t}}$ of -58%. Table II summarizes the statistical and leading systematic uncertainties on R and $\sigma_{t\bar{t}}$ excluding the 6.1% uncertainty on the integrated luminosity [18].

The total uncertainty on R is about 9%, compared to 17% achieved in the previous measurement [6]. The largest uncertainty comes from the limited statistics. Since the b-tagging efficiency drives the distribution of the events among the b-tag subsamples and is strongly anticorrelated with R, the systematic uncertainty is dominated by the b-tagging efficiency estimation, responsible for $\sim$90% of the total systematic uncertainty.

The total uncertainty on $\sigma_{t\bar{t}}$, excluding luminosity, is $\sim$10.5%, representing a 30% improvement over the previous measurement [7] assuming $R = 1$. Part of the improvement results from a fourfold reduction in the systematic uncertainties due to b-tagging, which is mostly absorbed by the R measurement.

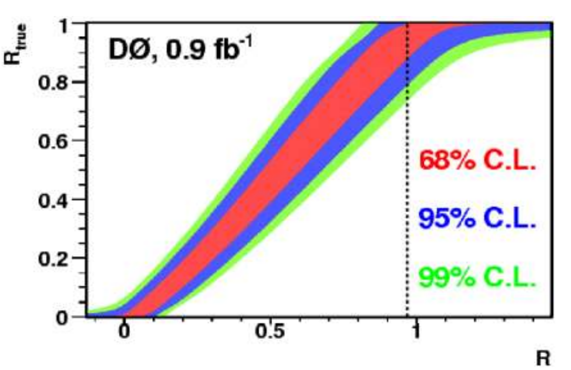

FIG. 2 (color online). The 68% (inner band), 95% (middle band), and 99% (outer band) C.L. bands for R_{true} as a function of R. The dotted black line indicates the measured value $R = 0.97$.

We extract a limit on R and $|V_{tb}|$ following the Feldman-Cousins procedure [19]. We generate pseudoexperiments with all systematic uncertainties included for various input values of R (R_{true}). We obtain $R > 0.88$ at 68% C.L. and $R > 0.79$ at 95% C.L., illustrated in Fig. 2. From R we determine the ratio of $|V_{tb}|^2$ to the off-diagonal matrix elements to be $\frac{|V_{tb}|^2}{|V_{ts}|^2+|V_{td}|^2} > 3.8$ at 95% C.L. Assuming a unitary CKM matrix with three fermion generations we derive $|V_{tb}| > 0.89$ at 95% C.L.

In summary, we have performed a simultaneous measurement of R and $\sigma_{t\bar{t}}$ yielding the most precise measurements to date, both in good agreement with the SM [1,20]. This measurement of R will be a key ingredient in a future model-independent direct determination of the $|V_{tq}|$ CKM matrix elements.

We thank the staffs at Fermilab and collaborating institutions, and acknowledge support from the DOE and NSF (USA); CEA and CNRS/IN2P3 (France); FASI, Rosatom and RFBR (Russia); CAPES, CNPq, FAPERJ, FAPESP and FUNDUNESP (Brazil); DAE and DST (India); Colciencias (Colombia); CONACyT (Mexico); KRF and KOSEF (Korea); CONICET and UBACyT (Argentina); FOM (The Netherlands); Science and Technology Facilities Council (United Kingdom); MSMT and GACR (Czech Republic); CRC Program, CFI, NSERC and WestGrid Project (Canada); BMBF and DFG (Germany); SFI (Ireland); The Swedish Research Council (Sweden); CAS and CNSF (China); Alexander von Humboldt Foundation; and the Marie Curie Program.

*Visitor from Augustana College, Sioux Falls, SD, USA.
†Visitor from The University of Liverpool, Liverpool, United Kingdom.
‡Visitor from ICN-UNAM, Mexico City, Mexico.
§Visitor from II. Physikalisches Institut, Georg-August-University, Göttingen, Germany.
‖Visitor from Helsinki Institute of Physics, Helsinki, Finland.
¶Deceased.

[1] N. Cabbibo, Phys. Rev. Lett. **10**, 531 (1963); M. Kobayashi and T. Maskawa, Prog. Theor. Phys. **49**, 652 (1973).
[2] W.-M. Yao *et al.*, J. Phys. G **33**, 1 (2006).
[3] V. Abazov *et al.* (D0 Collaboration), Phys. Rev. Lett. **98**, 181802 (2007).
[4] J. Alwall *et al.*, Eur. Phys. J. C **49**, 791 (2007).
[5] T. Affolder *et al.* (CDF Collaboration), Phys. Rev. Lett. **86**, 3233 (2001); D. Acosta *et al.* (CDF Collaboration), Phys. Rev. Lett. **95**, 102002 (2005).
[6] V. Abazov *et al.* (D0 Collaboration), Phys. Lett. B **639**, 616 (2006).

[7] V. Abazov *et al.* (D0 Collaboration), Phys. Rev. D **74**, 112004 (2006).
[8] D. Acosta *et al.* (CDF Collaboration), Phys. Rev. D **71**, 072005 (2005); A. Abulencia *et al.* (CDF Collaboration), Phys. Rev. Lett. **97**, 082004 (2006).
[9] V. Abazov *et al.* (D0 Collaboration), Nucl. Instrum. Methods Phys. Res., Sect. A **565**, 463 (2006).
[10] V. Abazov *et al.* (D0 Collaboration), Phys. Rev. D **76**, 092007 (2007).
[11] T. Scanlon, Ph.D. thesis, University of London, 2006.
[12] M. L. Mangano *et al.*, J. High Energy Phys. 07 (2003) 001.
[13] T. Sjöstrand *et al.*, arXiv:hep-ph/0308153.
[14] E. E. Boos *et al.*, Phys. At. Nucl. **69**, 1317 (2006).
[15] R. Brun and F. Carminati, CERN Program Library Long Writeup Report No. W5013, 1993 (unpublished).
[16] Z. Sullivan, Phys. Rev. D **70**, 114012 (2004); J. M. Campbell and R. K. Ellis, Phys. Rev. D **60**, 113006 (1999).
[17] The normalized momentum tensor, $\mathcal{M}$, is defined as $\mathcal{M}_{ij} = \frac{\Sigma_k p_i^k p_j^k}{\Sigma_k |\vec{p^k}|^2}$, where $\vec{p^k}$ is the momentum vector of a reconstructed object k, and i and j are Cartesian coordinates. Aplanarity $\mathcal{A}$, $\mathcal{C}_M$ and $\mathcal{D}_M$ are defined here as $\frac{3}{2}\lambda_3$, $3(\lambda_1\lambda_2 + \lambda_1\lambda_3 + \lambda_2\lambda_3)$ and $27\lambda_1\lambda_2\lambda_3$, respectively, where λ_1, λ_2, and λ_3 are the eigenvalues of $\mathcal{M}$.
[18] T. Andeen *et al.*, Fermilab Report No. FERMILAB-TM-2365, 2007.
[19] G. Feldman and R. Cousins, Phys. Rev. D **57**, 3873 (1998).
[20] N. Kidonakis and R. Vogt, Phys. Rev. D **68**, 114014 (2003); M. Cacciari *et al.*, J. High Energy Phys. 04, 68 (2004).